POLITECNICO DI TORINO
Repository ISTITUZIONALE

Localized-interaction-induced quantum reflection and filtering of bosonic matter in a one-dimensional lattice guide

Original
Localized-interaction-induced quantum reflection and filtering of bosonic matter in a one-dimensional lattice guide / Barbiero, L.; Malomed, B. A.; Salasnich, L.. - In: NEW JOURNAL OF PHYSICS. - ISSN 1367-2630. - ELETTRONICO. - 18:5(2016), p. 055007. [10.1088/1367-2630/18/5/055007]

Availability:
This version is available at: 11583/2948180 since: 2022-01-02T10:51:27Z

Publisher:
Institute of Physics Publishing

Published
DOI:10.1088/1367-2630/18/5/055007

Terms of use:

This article is made available under terms and conditions as specified in the corresponding bibliographic description in the repository

Publisher copyright

(Article begins on next page)

12 October 2024

New Journal of Physics
The open access journal at the forefront of physics

Deutsche Physikalische Gesellschaft DPG IOP Institute of Physics

PAPER • OPEN ACCESS

Localized-interaction-induced quantum reflection and filtering of bosonic matter in a one-dimensional lattice guide

To cite this article: L Barbiero *et al* 2016 *New J. Phys.* **18** 055007

View the article online for updates and enhancements.

You may also like

- Analytic Calculation of Arbitrary Matrix Elements for Boson Exponential Quadratic Operators
Pan Jianwei, Hou Guang and Zhang Yongde

- Decoding of intended saccade direction in an oculomotor brain–computer interface
Nan Jia, Scott L Brincat, Andrés F Salazar-Gómez et al.

- Associations between air pollution and psychiatric symptoms in the normative aging study
Xinye Qiu, Mahdieh Danesh-Yazdi, Marc G Weisskopf et al.

This content was downloaded from IP address 130.192.19.32 on 27/01/2022 at 11:46

New Journal of Physics
The open access journal at the forefront of physics

Deutsche Physikalische Gesellschaft DPG
IOP Institute of Physics

Published in partnership with: Deutsche Physikalische Gesellschaft and the Institute of Physics

CrossMark

OPEN ACCESS

RECEIVED
24 December 2015

REVISED
30 March 2016

ACCEPTED FOR PUBLICATION
25 April 2016

PUBLISHED
9 May 2016

Original content from this work may be used under the terms of the Creative Commons Attribution 3.0 licence.

Any further distribution of this work must maintain attribution to the author(s) and the title of the work, journal citation and DOI.

PAPER

Localized-interaction-induced quantum reflection and filtering of bosonic matter in a one-dimensional lattice guide

L Barbiero[1,5], **B A Malomed**[2] **and L Salasnich**[3,4,6]

[1] Dipartimento di Fisica e Astronomia 'Galileo Galilei', Università di Padova, I-35131 Padova, Italy
[2] Department of Physical Electronics, School of Electrical Engineering, Faculty of Engineering, Tel Aviv University, Tel Aviv 69978, Israel
[3] Dipartimento di Fisica e Astronomia 'Galileo Galilei' and CNISM, Università di Padova, I-35131 Padova, Italy
[4] INO-CNR, Research Unit of Sesto Fiorentino, Via Nello Carrara, I-1-50019 Sesto Fiorentino, Italy
[5] SISSA, via Bonomea 265, I-34136 Trieste, Italy
[6] Author to whom any correspondence should be addressed.

E-mail: luca.salasnich@unipd.it

Keywords: matter waves, Bose–Einstein condensates in periodic potentials, renormalization group methods

Abstract

We study the dynamics of quantum bosonic waves in a one-dimensional tilted optical lattice. An effective spatially localized nonlinear two-body potential barrier is set at the center of the lattice. This version of the Bose–Hubbard model can be realized in atomic Bose–Einstein condensates, with the help of localized optical Feshbach resonance, controlled by a focused laser beam, and in quantum optics, using an arrayed waveguide with selectively doped guiding cores. Our numerical analysis demonstrates that the central barrier induces anomalous quantum reflection of incident wave packets, which acts solely on bosonic components with multiple onsite occupancies, while single-occupancy components pass the barrier, allowing one to distill them in the interaction zone. As a consequence, in this region one finds a hard-core-like state, in which the multiple occupancy is forbidden. Our results demonstrate that this regime can be attained dynamically, using relatively weak interactions, irrespective of their sign. Physical parameters necessary for the experimental implementation of the setting in ultracold atomic gases are estimated.

1. Introduction

Isolated quantum systems in out-of-equilibrium configurations have attracted a great deal of interest due to the possibility of observing new quantum effects [1]. An ideal platform to build such systems is offered by ultracold bosons in reduced dimensionality [2–4], where all parameters of the system can be controlled with a high level of accuracy and flexibility [5]. In this context, the band structure generated by optical lattices (OLs) [6] and the absence of dissipation have allowed the experimental observation of peculiar out-of-equilibrium effects [7–9] predicted several years ago [10]. Atomic motion induced by tilted OL potentials has been widely explored too, revealing remarkable quantum features [11, 12]. Furthermore, the study of the dynamics of bosonic waves in a continuous geometry opens the way to a novel applications in nonlinear optics [13, 14] and plasmas [15]. Scattering of bosonic solitary matter waves on narrow repulsive [16–21] and attractive [22, 23] potential barriers or wells has been extensively studied in a theoretical form too, suggesting experimental observations of the effect of the quantum reflection [24, 25]. In early work [26] and more recently [14, 27, 28], configurations where effective *nonlinear* potential barriers or wells are induced by spatially localized two-body interaction have been proposed as a possible mechanism to observe other various forms of the anomalous reflection and splitting [29].

In this work we combine the above-mentioned ingredients to study the scattering of wave packets, composed of non-interacting bosons in a tilted OL, on a localized interaction zone, by means of systematic simulations based on the time-dependent density-matrix-renormalization-group (t-DMRG) method. Exotic effects, such as selective quantum reflection, distillation and filtering, are revealed as a result of the scattering. In particular, we demonstrate that, even for a relatively small interaction strength, the nonlinear barrier acts as quantum filter, which almost completely reflects bosonic components with multiple onsite occupancies, while

© 2016 IOP Publishing Ltd and Deutsche Physikalische Gesellschaft

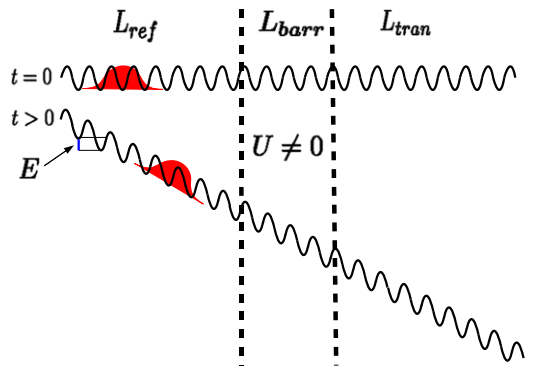

Figure 1. The setting under the consideration. At $t = 0$, a bosonic wave packet is placed at the edge of the left part of the lattice, of size $L_{\rm ref}$ (in terms of the number of the OL sites), into which a part of the wave packet is *reflected* after the collision with the interaction zone ($U \neq 0$). At $t > 0$, the evolution of the input is governed by Hamiltonian (1), with tilt E driving the particles towards the central interaction zone (nonlinear *barrier*) of size $L_{\rm barr}$. Adjacent to it on the right-hand side, is a part composed of $L_{\rm tran}$ OL sites, into which *transmitted* particles will move.

the components carrying the single occupancy (SO) are able to pass the barrier. In this way, a region where multiple occupancies (MO) are forbidden is found. We demonstrate that such a state can be *distilled* from the incident wave packet, using both repulsive and (rather unexpectedly) attractive localized interactions. Furthermore, our analysis reveals that the distillation effect, induced by the lattice's band structure, features its most pronounced form, i.e., the total MO reflection, at relatively small interaction strengths, and it is not essentially affected by variation of the potential tilt which drives the incident wave packets.

2. The model

We study the evolution of an initially localized bosonic wave packet moving in a one-dimensional (1D) tilted OL, with onsite interaction acting in a finite region ('barrier') of size $L_{\rm barr}$ (measured in terms of the OL sites), where a part of incident waves may be trapped in the case of the attractive interaction, see figure 1. At $t = 0$, we place a Gaussian wave packet near the left edge of the whole lattice. Experimentally, the initial packet may be created by a very tight harmonic-oscillator trap, initially applied at the same spot, which is subsequently lifted. Potential tilt E can be produced and tuned by applying dc magnetic field along the vertical direction, with a gradient along the OL, its effect being to induce the accelerated motion of atoms towards the center, where a zone representing the nonlinear scatterer [26, 27, 29] is composed of a finite number of sites carrying onsite interaction strength ($U \neq 0$).

Spatially non-uniform interactions in ultracold atomic gases were recently realized in experiments [30–32], with the help of the Feshbach resonance controlled by inhomogeneous external fields. These results motivate the consideration of various settings based on effective nonlinear potentials [26, 27, 29, 33–36], which includes the prediction of 1D quantum solitons in the Bose–Hubbard (BH) model with the strength of the onsite repulsive interaction ($U_i > 0$) growing with the distance from the center, $|i|$, at any rate faster than $|i|$ [37]. On the other hand, it was shown in detail in the context of another physical setting in [29] that a confined interaction zone, extending over the width corresponding to a few OL sites, can be induced by means of the optical Feshbach resonance controlled by a laser beam shone onto the lattice in the perpendicular direction.

Here we consider the evolution of the atomic condensate governed by the following Hamiltonian of the BH type:

$$H = -J\sum_{i=1}^{L}(b_i^\dagger b_{i+1} + b_{i+1}^\dagger b_i) + \frac{U}{2}\sum_{i=L_{\rm ref}+1}^{L_{\rm ref}+L_{\rm barr}} n_i(n_i - 1) - E\sum_{i=1}^{L} i\, n_i, \tag{1}$$

where b_i ($b_i^\dagger$) is the bosonic annihilation (creation) operator for an atom at the ith site in the lattice of total length L, and n_i is the atomic population at the site. The hopping of atoms between nearest lattice sites is controlled, as usual, by the respective probability J, which sets scales for energy and time in the present system (i.e., $J = 1$ is set below), E is the potential tilt, and U the strength of the two-body interaction at those sites where it is present, i.e., $L_{\rm ref} + 1 \leqslant i \leqslant L_{\rm ref} + L_{\rm barr}$. Since we apply the interaction in a small part of the lattice, it is relevant to distinguish three different regions: the left region with $L_{\rm ref}$ sites, into which the incident atoms are reflected, the central region of the nonlinear barrier with $L_{\rm barr}$ sites, and the right region with $L_{\rm tran}$ sites, into which the atoms may be transmitted. Thus, the total number of sites in the lattice, which as a whole is embedded into a potential box, is $L = L_{\rm ref} + L_{\rm barr} + L_{\rm tran}$, as shown in figure 1.

To estimate a possibility of the experimental implementation of the proposed setting in ultracold gases, it is relevant to refer to recent experimental work [38], which used cesium atoms in the hyperfine ground state, $|F = 3,\ m_F = 3\rangle$, for realizing regular and chaotic regimes of the superfluid flow in tilted OLs, created by laser beams with wavelength $\lambda = 1.0645\ \mu$m, with the corresponding depth equal to seven recoil energies ($E_{\rm recoil} = 1.325$ kHz). This value of the depth translates into the atom's hopping rate $J = 52.3$ Hz. Further, the scattering length $a_s = 21.4\ a_0$ corresponds to the onsite interaction strength $U = 102$ Hz, which, by means of the Feshbach resonance, could be increased up to $U = 533$ Hz. Thus, the setting made it possible to easily realize values of the main control parameter, U/J, ranging between 2 and 5. Values of this parameter which are essential to the results reported below are virtually the same, $2 < U/J < 6$. The potential ramp was created in [38] using a combination of gravity and magnetic-field gradient, with values up to $\nabla B = 31.1$ G cm^{-1}. This method makes it possible to readily adjust values of E/J to values relevant to the present analysis, which are $0.1 < E/J < 0.5$, see below.

In addition to atomic Bose–Einstein condensates, the same BH system may be implemented as a quantum-optics model of an array of evanescently coupled parallel waveguides [39] (possibly, photonic nanowires [40]). In that case, the localized interaction zone can be created by means of selectively doping the respective guiding cores by a material which resonantly enhances the Kerr nonlinearity [41], while the potential ramp can be used by tapering individual cores. In the optics model, the evolution variable, t, is replaced by the propagation distance, z. Typically, the hopping rate corresponds to the inter-core coupling length $J^{-1} \lesssim 1$ cm, which makes it necessary to have the nonlinearity length as short as $U^{-1} \sim 2$ mm. This value is challenging, but the us of the resonantly enhanced nonlinearity may make it possible.

3. Numerical results

We report numerical results obtained by means of the t-DMRG technique [42] using 350 DMRG states in the time-evolution calculations and time step $\Delta t = 0.01$ (it was checked that taking smaller Δt does not affect the results). We simulated the system with $L = 20$ lattice sites and a variable number N of bosons, fixing the corresponding sizes in equation (1) as $L_{\rm ref} = L_{\rm tran} = 8$ and $L_{\rm barr} = 4$. Although the total size used here, $L = 20$, is relatively small, it is comparable with that in experimentally realized systems [43] . It can be checked that the increase of L and, accordingly, of $L_{\rm ref}$, $L_{\rm barr}$, $L_{\rm tran}$ affects only characteristic time scales of the dynamical results reported below, but does not essentially alter outcomes of the scattering.

3.1. The flat repulsive barrier

Usually, reflection and transmission of wave packets is revealed by tracking expectation values $\langle n_i\rangle$ of the density profile with respect to the evolving many-body quantum state, $|\psi(t)\rangle$. Note that $\langle n_i\rangle$ can be precisely measured in the experiment, by means of the recently developed *in situ* imaging technique [44, 45]. The Gaussian shape of $\langle n_i\rangle$ at $t = 0$ is localized on five lattice sites populated by $N = 8,\ 10,\ 12$ bosons, respectively, in the first, second and third row of figure 2. Once at $t > 0$ the bosons are free to move toward the central part of the system, the initial Gaussian density profile is deformed[7], and its actual shape depends on N, as is evident in the first column of figure 2.

Figures 2(a), (d) and (g) show typical quantum-reflection effects for $E = 0.3$ and $U = 6.0$. Indeed, it is seen that, as the bosons approach the interaction zone[8] with $U \neq 0$, a large fraction of them bounce back, with only a small part being able to pass $L_{\rm barr}$. At the first glance, this behavior is similar to the one induced by the usual linear potential barrier, see, e.g., [25]. However, a crucial difference is that the *nonlinear* (interaction-induced) barrier in our setting acts only on two- and many-body states. Therefore, it is necessary to distinguish between the SO and MO scattering behaviors. To this end, we define two operators acting on the many-body quantum state, $|\psi(t)\rangle$. One operator counts SO sites, with occupancy $\langle n_i\rangle \leqslant 1$:

$$n_i^{\rm s}\ |\psi(t)\rangle = \alpha\ |\psi(t)\rangle \quad \text{with} \quad \alpha = \langle n_i\rangle \quad \text{if} \quad \langle n_i\rangle \leqslant 1, \ \text{and} \quad \alpha = 0 \quad \text{if} \quad \langle n_i\rangle > 1. \tag{2}$$

The operator counting MO sites is $n_i^{\rm p} = n_i(n_i - 1)/2$, which acts according to

$$n_i^{\rm p}\ |\psi(t)\rangle = \beta\ |\psi(t)\rangle \quad \text{with} \quad \beta = 0 \quad \text{if} \quad \langle n_i\rangle \leqslant 1, \ \text{and} \quad \beta = \langle n_i(n_i - 1)\rangle/2 \quad \text{if} \quad \langle n_i\rangle > 1. \tag{3}$$

Thus we can separately take into account sites where the interaction, if present, is effective, i.e. $\langle n_i^{\rm p}\rangle \neq 0$, and where it is not, i.e., $\langle n_i^{\rm s}\rangle \neq 0$. In the second and third columns of figure 2, respectively, we show the evolution of the expectation values of operators n_i^s and n_i^p . While it is evident from figures 2(b), (e), and (h) that the SO, represented by $\langle n_i^{\rm s}\rangle$, freely passes the nonlinear barrier, figures 2(c), (f), and (i) make it clear that the MO,

[7] In a tilted lattice the motion of a wave packet with a permanent shape is impossible due to the constrain imposed by the energy conservation.

[8] In all the cases shown, the $U \neq 0$ term is located only at sites with $i = 9,\ 10,\ 11,\ 12$.

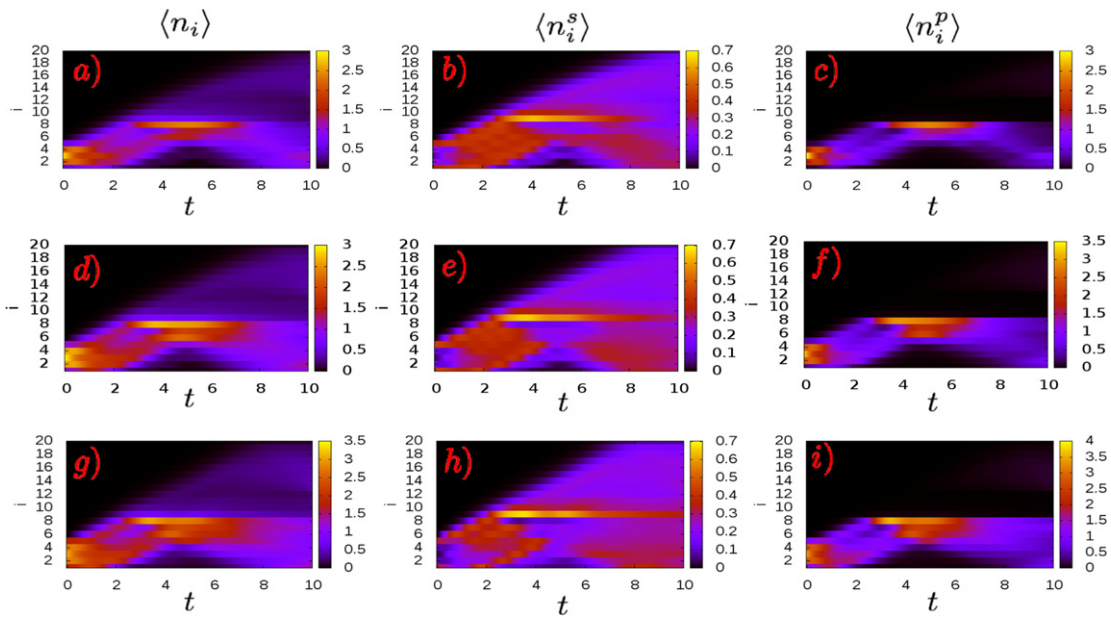

Figure 2. The first, second and third columns show the evolution of $\langle n_i \rangle$, $\langle n_i^s \rangle$, and $\langle n_i^p \rangle$, respectively. The single- and multiple-occupancy expectation values, $\langle n_i^s \rangle$ and $\langle n_i^p \rangle$, are produced by the operators defined in equations (2) and (3), respectively. They are evaluated in the system with $N = 8,\ 10$, and 12 bosons, in the first, second and third rows, respectively. All the results refer to a lattice with $L = 20$ sites, with N bosons placed at $t = 0$ on 5 lattice sites. The other parameters are $L_{\rm ref} = L_{\rm tran} = 8$, $L_{\rm barr} = 4$, $U = 6.0$, and $E = 0.3$.

represented by $\langle n_i^{\rm p} \rangle$, bounces back from it. More precisely, we notice that, after an initial decrease due to the propagation in the non-interaction regime, $\langle n_i^{\rm p} \rangle$ consistently grows at the right edge of $L_{\rm ref}$ at intermediate times. The accumulation of the MO is followed by its nearly complete rebound. On the other hand, the SO features the behavior reverse to that of $\langle n_i^{\rm p} \rangle$ in the $L_{\rm ref}$ section of the lattice. In particular, dissociation (formation) of the MO is coupled to the increase (decrease) of $\langle n_i^s \rangle$.

The crucial point is the behavior of the bosons inside the central interaction zone, where, on the contrary to the MO, the SO can evidently reside. This fact is a drastic difference with respect to the usual settings, with a linear-potential barrier acting at the single-particle level. Thus, as already stated, the quantum transmission observed in figures 2(a), (d), and (g) is totally accounted for by the SO motion. In other words, the interaction zone acts as a *quantum filter*, which sends all the occupancies with $\langle n_i \rangle > 1$ back, and lets those with $\langle n_i \rangle < 1$ pass. In this way, the interaction zone, cleared of the MO, displays an effective hard-core on-site repulsion, with bosonic particles emulating fermions. A quantum gas where the pair- and multiple-occupations are forbidden due to the interaction is usually associated to the appearance of the Tonks–Girardeau (TG) regime. The latter was originally predicted in a configuration preserving the Galilean invariance [46–48], but it has later been demonstrated both theoretically [49] and experimentally [50] that the presence of a lattice preserves the main features of the TG gas. Noticeably, in figure 2 the hard-core constraint is generated for all considered values of the boson number, N. The latter fact signals that the interaction strength, U, is responsible for the filtering effect. To check the efficiency of the filter, in figure 3 we plot densities which are, respectively, the observation values of n_i, $n_i^{\rm p}$ and n_i^s, averaged over three different parts of the lattice, $L_{\rm r,t,t} \equiv \{L_{\rm ref},\ L_{\rm barr},\ L_{\rm tran}\}$, for different values of the interaction strength, U:

$$\rho = L_{\rm r,b,t}^{-1} \sum_{L_{\rm r,b,t}} \langle n_i \rangle, \qquad \rho_{\rm p} = L_{\rm r,b,t}^{-1} \sum_{L_{\rm r,b,t}} \langle n_i^{\rm p} \rangle, \qquad \rho_{\rm s} = L_{\rm r,b,t}^{-1} \sum_{L_{\rm r,b,t}} \langle n_i^s \rangle. \tag{4}$$

It is clearly seen in figure 3 that, in the course of the evolution the value of $\rho_{\rm p}$ is conspicuously different from zero in region $L_{\rm barr}$ only for a relatively weak interaction strength, namely, $U = 2$. Once a stronger interaction acts in $L_{\rm barr}$, the MO density practically vanishes. As a result, at intermediate values of time, a gas composed of the SO is stabilized in the distilled form inside the interaction zone. Obviously, the number of particles approaching the barrier does not depend on the interaction strength present in $L_{\rm barr}$, as is evident in the first column of figure 3. In the same time, once the interaction capable to support the quantum filtering is applied in $L_{\rm barr}$, the value of $\rho_{\rm s}$ becomes independent of the interaction strength U. This is confirmed by the fact that in figure 3 we see that, for $U = 4$ and 6, $\rho_{\rm p}$ is actually zero in region $L_{\rm barr}$, hence $\rho_{\rm s}$ has the same value for these two interaction strengths. As seen in the third column of figure 3, this aspect has its consequences also in the behavior of bosons in region $L_{\rm tran}$. Indeed, the filtering process allows a larger number of bosons to enter $L_{\rm tran}$, which means that, effectively,

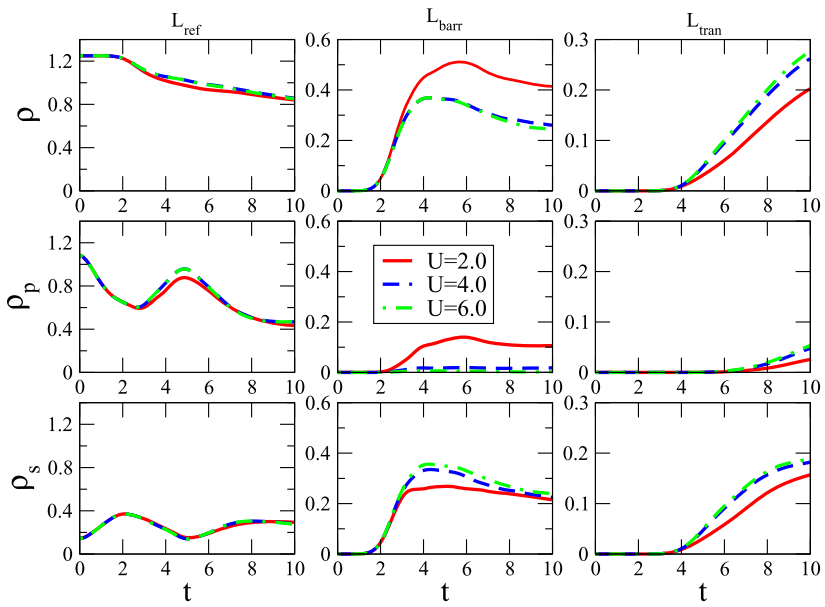

Figure 3. The three rows display, respectively, the evolution of average densities of the total number of bosons, SO (single occupancy), and MO (multiple occupancy), in the three sections of the lattice, which are defined as per equation (4). The three columns refer to sections L_{ref}, L_{barr} and L_{tran}, as indicated in the top line. The data were collected for $N = 10$ bosons and $L = 20$ sites, with N bosons placed, at $t = 0$, on 5 lattice sites. The other parameters are $L_{\mathrm{ref}} = L_{\mathrm{tran}} = 8$, $L_{\mathrm{barr}} = 4$, $E = 0.3$, and different values of U, as indicated in the figure.

the dynamically induced hard-core constraint increases the speed of the particles. In particular, our measurements yield $\rho(U = 4,\ 6)/\rho(U = 2) \approx 1,\ 25$ at $t = 10$. Interestingly this larger amount of particles allows the formation of higher SO and MO alike, see values of ρ_{s} and ρ_{p} in the third column of figure 3.

3.2. The flat attractive barrier

The quantum reflection of the MO might seem a rather obvious consequence of the repulsive nature of the interaction. For this reason, it is interesting to consider the system with attractive interactions, i.e., $U < 0$, too. The analysis of static configurations for $U < 0$ and relatively large $|U|$ has previously revealed collapsed states, see [27, 51] and references therein. This fact suggests that MO may not bounce back from the interaction zone, L_{trap}, and get partly trapped in it. Nevertheless, figure 4, which displays the same characteristics of the dynamical scattering as in figure 3, but for $U < 0$, shows that this *does not happen*—in fact, the self-attraction zone does not accumulate the MO. Actually we observe that this system again stabilizes an effectively 'distilled' quasi-TG state in this zone, although with a higher density than in the case of $U > 0$.

The approximate symmetry between the cases of $U > 0$ and $U < 0$, revealed by the comparison of figures 3 and 4, agrees with findings of [52], where a similar symmetry was discovered in the transport of fermion atoms. In the present contexts, it is related to properties of the energy spectrum of lattice bosons, which demonstrates the symmetry with respect to $U \leftrightarrow -U$. Moreover, the consideration of the attractive interaction helps one to understand how the present BH model gives rise to the quantum filtering, distillation, and rebound effects. First, it is obvious that, in either case, the system conserves the total energy (along with the total number of bosons). Further, the band structure produced by the OL imposes a limitation on possible values of the kinetic energy. In fact, the formation of MO in the interaction zone would induce energy variation that cannot be supported by the system in which any gain/loss in the potential energy must be converted into the opposite change of the kinetic energy. A precise many-body quantification of this effect is a very hard problem, due to the non-integrability of equation (1). Nevertheless, arguments regarding the two- [7–9] and three-body [53] bound states may be sufficient to explain many significant dynamical quantum effects in 1D lattice systems [7–9, 54]. In our case, the derivation of the two- and three-body energy spectrum is substantially complicated by the presence of the tilted potential. Nevertheless, the same energy arguments make it possible to explain the above-mentioned effect.

Actually, the rebound of the MO bosonic component from the self-attraction region, observed in figure 4, is alike to the commonly known effect of the partial reflection of an incident wave from a quantum-mechanical potential well [55], and also to the possibility of the rebound of a moving soliton from a potential well in the nonlinear model [56].

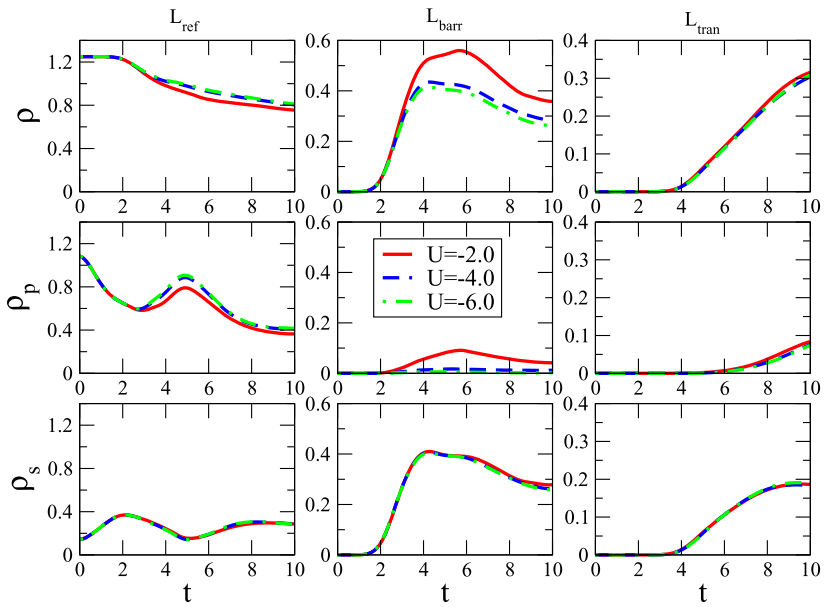

Figure 4. The same as in figure 3, but for the system with the attraction ($U < 0$) acting in the interaction zone ($L_{\rm barr}$).

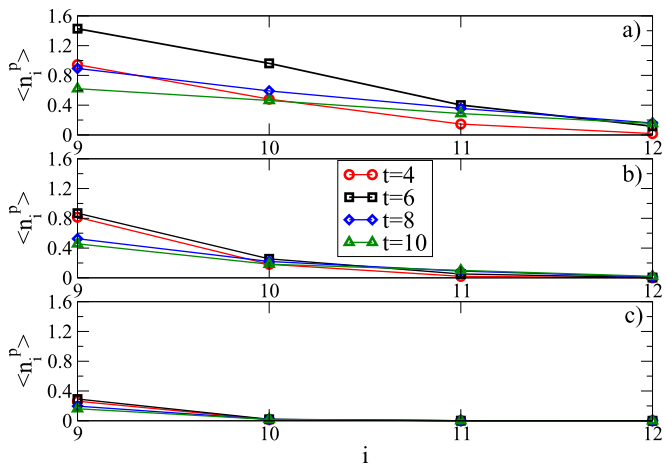

Figure 5. The expectation value of $\langle n_i^{\rm p}\rangle$ in region $L_{\rm barr}$, namely, at sites $i = 9,\ 10,\ 11,\ 12$, in the system with $N = 10$ bosons initially placed on 5 lattice sites, and $E = 0.3$. The local interaction strength, $U(i) = U_{\rm min}\cdot(i-8)$, grows linearly with the distance, with slope $U_{\rm min} = 0.5,\ 1.0$, and 2.0 in (a), (b) and (c), respectively.

3.3. A linearly shaped repulsive barrier

All the results presented above refer to a configuration where the bosons are subject to spatially uniform interactions in region $L_{\rm barr}$. A essential issue is whether a barrier with spatially inhomogeneous interactions gives rise to similar filtering effects.

In figure 5 we show the behavior of $\langle n_i^{\rm p}\rangle$, evaluated at different times in region $L_{\rm barr}$ in the system with the interaction strength growing linearly with the distance. More precisely, we study a configuration where the bosons are subject to the site-dependent interaction $U(i)$, with minimum value $U_{\rm min}$ at site $i = 9$, and maximum strength $U_{\rm max}$ at $i = 12$, i.e. $U(i) = U_{\rm min}(i-8)$. As might be expected, it is observed in figure 5(a), corresponding to $U_{\rm min} = 0.5$, that such a weak potential is not able to support any filtering. Noticeably, at site $i = 12$, where the strength is $U(i = 12) = 2$, we find that $\langle n_i^{\rm p}\rangle$ has the same value of $\rho_{\rm p}$ as evaluated in region[9] $L_{\rm barr}$ in figure 3 for $U = 2$. A similar feature is shown in figure 5(b), where $U_{\rm min} = 1$. Here we note that, at site $i = 10$, where $U(10) = 2$, we again find the same value of $\rho_{\rm p}$, averaged over $L_{\rm barr}$, as in figure 3 for $U = 2$. Moreover, it is relevant to point out that the only site where MO is actually forbidden is the point where

[9] Note that we are here referring to the value of $\langle n_i^{\rm p}\rangle$ at the ith site. It actually corresponds to having the barrier with interaction constant $U = 2$ on one lattice site. For this reason, we have $\langle n_i^{\rm p}\rangle = \rho_{\rm p}$ following the definition of (4).

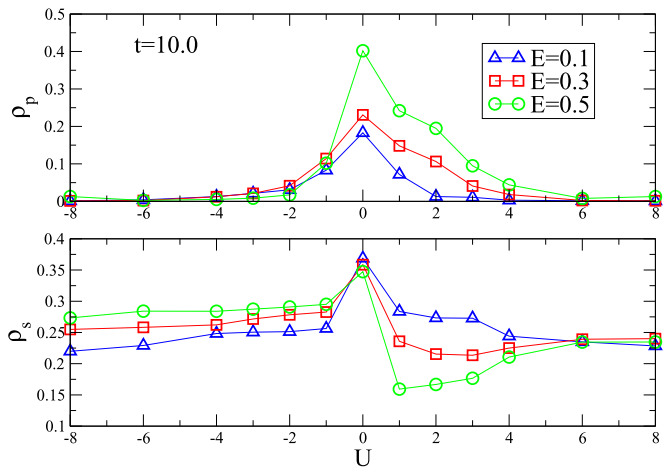

Figure 6. Average MO and SO densities, ρ_p and ρ_s, in the interaction zone, defined as per equation (4) (with $L_{r,t,t} = L_{barr}$), taken at $t = 10$, as functions of the interaction strength U, at different fixed values of the potential tilt, E. Initially, $N = 10$ bosons are placed on 5 lattice sites.

$U(i = 12) = 4$, again in agreement with figure 3 for $U = 4$. Finally, the same correspondence with figure 3 is observed in in figure 5(c), where $U_{min} = 2$. Here, the strong interaction produces filtering effects at all sites but $i = 9$, where the local interaction strength is not strong enough, $U(9) = 2$. Notice that the number of particles and single-/multiple-occupations at $i > 12$ is exactly the same as in the case of the flat barrier. In particular, the state at $i > 12$ for $U_{min} = 0.5$ is exactly the same as that observed in column 3 of figure 3 (the red curve).

Finally, we make conclusions for the present case. First , we conclude, as expected, that the only ingredient generating the filtering is the strength of the interaction, but not its spatial distribution. Moreover, the comparison of figures 3 and 5 makes it clear that the size of the interaction zone does not play any role in the generation of the effective hard-core constraint on the MO. More precisely, the larger is the number of sites with sufficiently strong interaction, the broader is the region where the effective hard-core repulsion is present.

3.4. Different initial configurations

As pointed out above, the energy considerations determine the filtering and reflection effects outlined above. Actually, the energy of the initial state in equation (1) depends on several parameters, such as the potential tilt, E, the spatial extension of the wave packet at $t = 0$, and the number of bosons, N, which is the crucial quantity controlling the effects described above. For this reason, it is relevant to explore how different initial configurations affect our findings. As clearly seen in figure 1, a small variation of N does not bring any conspicuous variation in the filtering properties. A different role is played by E. The respective results are displayed in figure 6, where we plot the average MO and SO densities, ρ_p and ρ_s, in the interaction zone for different values of E at a fixed evolution time, $t = 10$. The figure clearly shows that the MO density in the interaction zone is conspicuously affected by E only at sufficiently small values of the interaction strength[10], $|U|$, while ρ_p practically vanishes at larger values of $|U|$.

On the other hand, the average SO density in the interaction zone, ρ_s, shows a weak dependence on E at almost all values of U, as shown in the lower panel of figure 6, suggesting that E can be used to adjust the density of the TG state 'distilled' in the interaction zone. We thus conclude that the effects of the quantum filtering and MO reflection persist in the present version of the BH system at small and intermediate values of E. On the contrary, the situation becomes trivial at large E, when the potential ramp becomes a dominant factor determining the dynamics of the wave packets. Finally, in figure 7 we display the evolution of $\langle n_i^p \rangle$ for wave packets initially localized on different numbers of sites, but with the same number of particles, $N = 10$.

Thus, we infer that the variation induced by a difference in the localization of the initial density profile does not cause any appreciable modification of the physical features described above. Of course, much larger variations in the number of the initially occupied sites may alter the critical value of U which gives rise to the effective hard-core behavior. Nevertheless, we conclude that, due to energy considerations, it is always possible, in the 1D isolated quantum system, to find a critical strength of the interaction able to give rise to the filtering precesses.

[10] Actually we observe that the value of ρ_p is more affected by U in the case of the repulsive interaction.

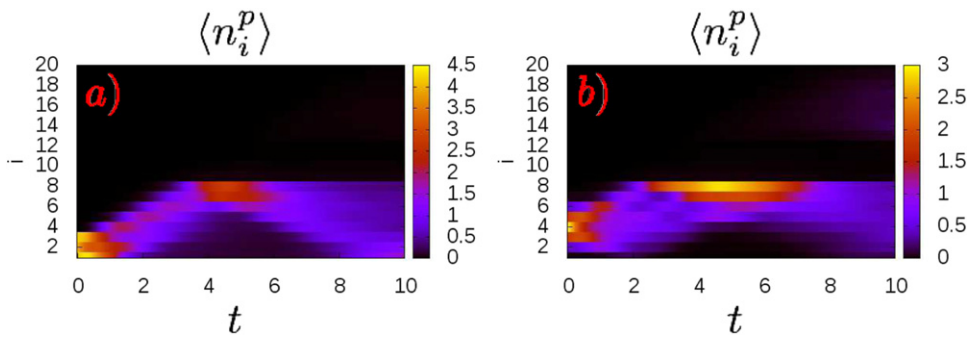

Figure 7. Evolution of $\langle n_i^{\mathrm{P}} \rangle$ in the system with $N = 10$, $E = 0.3$, and $U = 6$ in the central part of the lattice. (a) and (b) refer to a configuration where the initial Gaussian profile is localized over 3 or 7 sites, respectively.

4. Conclusion

We have introduced a version of the BH system composed of two sections which do not carry onsite two-body interactions, with an interaction zone sandwiched between them. The cases of spatially uniform repulsive and attractive interactions, as well as inhomogeneous interactions, were considered. This is a fully quantum counterpart of models with nonlinear potential barriers or wells, that were recently studied in optics and mean-field description of matter waves in atomic BEC. In those contexts, the spatially localized interactions may be induced, respectively, by means of selective doping, or by the Feshbach resonance controlled by an inhomogeneous external field. Using the quasi-exact numerically implemented t-DMRG method, we have considered the scattering problem, where the potential tilt sends a wave packet to collide with the effective nonlinear barrier (interaction zone). The result is that the nonlinear barrier, being transparent to the bosonic-wave component with the onsite SO, induces strong quantum reflection of the MO (multiple-occupancy) bosonic components. These properties make it possible to realize the quantum distillation of the SO component in the interaction zone, which is tantamount to inducing an effective on-site hard-core repulsion. The absence of the MO, which was experimentally demonstrated to be a characteristic feature of the TG state [50, 57], makes it possible to dynamically realize a similar state in the interaction zone of the present system. Furthermore, we have shown that, in contrast to the static configuration, where the hard-core regime occurs for very strong repulsive interaction (while strong attraction may generate a highly excited state in the form of the super-TG gas [58–61]), our dynamical setting makes it possible to reach this hard-core-like regime, using relatively weak repulsion, or even weak attraction (which is an unexpected finding), in the interaction zone. Further investigations are currently in progress, to better characterize this peculiar regime. It has been demonstrated that the predicted results can be implemented using currently available experimental settings.

Acknowledgments

We appreciate a valuable discussion with M D Lukin. This work was supported by MIUR (FIRB 2012, Grant No. RBFR12NLNA-002; PRIN 2013, Grant No. 2010LLKJBX). L B thanks CNR-INO BEC Center in Trento for CPU time.

References

[1] Polkovnikov A, Sengupta K, Silva A and Vengalattore M 2011 *Rev. Mod. Phys.* **83** 863
[2] Salasnich L, Parola A and Reatto L 2002 *Phys. Rev.* A **65** 043614
[3] Mateo Muñoz A and Delgado V 2008 *Phys. Rev.* A **77** 013617
[4] Cazalilla M A, Citro R, Giamarchi T, Orignac E and Rigol E 2011 *Rev. Mod. Phys.* **83** 1405 and references therein
[5] Bloch I, Dalibard J and Zwerger W 2008 *Rev. Mod. Phys.* **80** 885
[6] Jaksch D, Bruder C, Cirac J I, Gardiner C W and Zoller P 1998 *Phys. Rev. Lett.* **81** 3108
[7] Winkler K, Thalhammer G, Lang F, Grimm R, Hecker-Denschlag J, Daley A J, Kantian A, Büchler A P and Zoller P 2006 *Nature* **441** 853
[8] Strohmaier N, Greif D, Jördens R, Tarruell L, Moritz H, Esslinger T, Sensarma R, Pekker D, Altman E and Demler E 2010 *Phys. Rev. Lett.* **104** 080401
[9] Mark M J, Haller E, Lauber K, Danzl J G, Janisch A, Büchler H P, Daley A J and Nägerl H C 2012 *Phys. Rev. Lett.* **108** 215302
[10] Hubbard J 1963 *Proc. R. Soc.* A **276** 238
[11] Simon J, Bakr W S, Ma R, Tai M E, Preiss M P and Greiner M 2011 *Nature* **472** 307
[12] Meinert F, Mark M J, Kirilov E, Lauber K, Weinmann P, Gröbner M, Daley A J and Nägerl H C 2014 *Science* **344** 1259–62
[13] Kivshar Y S and Agrawal G 2003 *Optical Solitons: From Fibers to Photonic Crystals* (San Diego, CA: Academic)
[14] Kartashov Y V, Malomed B A and Torner L 2011 *Rev. Mod. Phys.* **83** 247

[15] Stasiewicz K, Shukla P K, Gustafsson G, Buchert S, Lavraud B, Thide B and Klos Z 2003 *Phys. Rev. Lett.* **90** 085002
[16] Helm J L, Billam T P and Gardiner S A 2012 *Phys. Rev.* A **85** 05362
[17] Martin A D and Ruostekoski J 2012 *New J. Phys.* **14** 043040
[18] Cuevas J, Kevrekidis P G, Malomed B A, Dyke P and Hulet R 2013 *New J. Phys.* **15** 063006
[19] Polo J and Ahufinger V 2013 *Phys. Rev.* A **88** 053628
[20] Helm J L, Rooney S J, Weiss C and Gardiner S A 2014 *Phys. Rev.* A **89** 033610
[21] Helm J L, Cornish S L and Gardiner S A 2015 *Phys. Rev. Lett.* **114** 134101
[22] Lee C and Brand J 2006 *Eur. Phys. Lett.* **73** 321
[23] Ernst T and Brand J 2010 *Phys. Rev.* A **81** 033614
[24] Marchant A L, Billam T P, Wiles T P, Yu M M H, Gardiner S A and Cornish S L 2013 *Nat. Commun.*s **4** 1865
[25] Marchant A L, Billam T P, Yu M M H, Rakonjac A, Helm J L, Polo J, Weiss C, Gardiner S A and Cornish S L 2016 *Phys. Rev.* A **93** 021604
[26] Malomed B A and Ya Azbel M 1993 *Phys. Rev.* B **47** 10402
[27] Dror N and Malomed B A 2011 *Phys. Rev.* A **83** 033828
[28] Maor O, Dror N and Malomed B A 2013 *Opt. Lett.* **38** 5454
[29] Sakaguchi H and Malomed B A 2016 *New J. Phys.* **18** 025020
[30] Bauer D M, Lettner M, Vo C, Rempe G and Dürr S 2009 *Nature Phys.* **5** 339
[31] Yamazaki R, Taie S, Sugawa S and Takahashi Y 2010 *Phys. Rev. Lett.* **105** 050405
[32] Clark L W, Ha L-C, Xu C-Y and Chin C 2015 *Phys. Rev. Lett.* **115** 155301
[33] Mayteevarunyoo T, Malomed B A and Dong G 2008 *Phys. Rev.* A **78** 053601
[34] Borovkova O V, Kartashov Y V, Malomed B A and Torner L 2011 *Opt. Lett.* **36** 3088
[35] Borovkova O V, Kartashov Y V, Torner L and Malomed B A 2011 *Phys. Rev.* E **84** 035602(R)
[36] Gligorić G, Maluckov A, Hadzievski L and Malomed B A 2013 *Phys. Rev.* E **88** 032905
[37] Barbiero L, Malomed B A and Salasnich L 2014 *Phys. Rev.* A **90** 063611
[38] Meinert F, Mark M J, Kirilov E, Lauber K, Weinmann P, Grobner M and Näger H C 2014 *Phys. Rev. Lett.* **112** 193003
[39] Krimer D O and Khomeriki R 2011 *Phys. Rev. A* **84** 041807
[40] Ye F, Mihalache D, Hu B and Panoiu N C 2010 *Phys. Rev. Lett.* **104** 106802
[41] Hukriede J, Runde D and Kip D 2003 *J. Phys. D: Appl. Phys.* **36** R1
[42] White S R and Feiguin A E 2004 *Phys. Rev. Lett.* **93** 076401
White S R and Feiguin A E 2005 *Phys. Rev.* B **72** 020404(R)
[43] Fukuhara T, Schauss P, Endress M, Hild S, Cheneau M, Bloch I and Gross C 2013 *Nature* **502** 76
[44] Bakr W S, Gillen J I, Peng A, Foelling S and Greiner M 2009 *Nature* **462** 74
[45] Sherson J F, Weitenberg C, Endres M, Cheneau M, Bloch I and Kuhr S 2010 *Nature* **467** 68
[46] Tonks L 1936 *Phys. Rev.* **50** 955
[47] Bijl A 1936 *Physica* **4** 329
[48] Girardeau M 1960 *J. Math. Phys.* **1** 516
[49] Cazalilla M A 2003 *Phys. Rev.* A **67** 053606
Cazalilla M A 2004 *Phys. Rev.* A **70** 041604(R)
[50] Paredes B, Widera A, Murg V, Mandel O, Fölling S, Cirac I J, Shlyapnikov G W, Hansch T W and Bloch I 2004 *Nature* **429** 277
[51] Barbiero L and Salasnich L 2014 *Phys. Rev.* A **89** 063605
[52] Schneider U *et al* 2012 *Nat. Phys.* **8** 213
[53] Johnson R, Tiesinga E, Porto J V and Williams C J 2009 *New J. Phys.* **11** 093022
[54] Barbiero L, Menotti C, Recati A and Santos L 2015 *Phys. Rev.* B **92** 180406(R)
[55] Landau L D and Lifshitz E M 1974 *Quantum Mechanics* (Moscow: Nauka)
[56] Ernst T and Brand J 2010 *Phys. Rev.* A **81** 033614
[57] Kinoshita H, Wenger T T and Weiss D S 2004 *Science* **305** 1125
[58] Chen S, Guan L, Yin X, Hao Y I and Guan X M 2010 *Phys. Rev.* A **81** 031609
[59] Muth D and Fleischhauer M 2010 *Phys. Rev. Lett.* **105** 150403
[60] Girardeau M D and Astrakharchik G E 2012 *Phys. Rev. Lett.* **109** 235305
[61] Panfil M, De Nardis J and Caux J-S 2013 *Phys. Rev. Lett.* **110** 125302